Fundamental Phase-matched Second Harmonic Generation from Mid-infrared to Near-infrared

Tianye Huang, Guizhen Xu, Jianxing Pan, Zhuo Cheng
School of Mechanical Engineering and Electronic Information
China University of Geosciences (Wuhan)
Wuhan, China
e-mail: tianye_huang@163.com

Shuwen Zeng
XLIM Research Institute
University of Limoges
Limoges CEDEX, France

Perry Shum Ping
Center of Fiber Technology, School of Electrical and Electronic Engineering
Nanyang Technological University
Singapore.

Gilberto Brambilla
Optoelectronics Research Centre
University of Southampton
Southampton, UK

***Abstract*—A polymer plasmonic waveguide for second harmonic generation (SHG) from mid-infrared (MIR) to near-infrared (NIR) is proposed. The required phase matching condition (PMC) is satisfied between the fundamental plasmonic mode at the fundamental frequency (FF) and the photonic mode at the second harmonic frequency (SHF). According to our simulations, the SHG conversion efficiency of 4.173% can be obtained in 92.3 μm length waveguide with 1 W pump power. Moreover, the conversion can be further enhanced by using a microring resonator (MRR). By optimizing the MRR, the SHG conversion efficiency can be increased to 26.1%. The proposed scheme can be a potential approach for MIR and NIR wavelength conversion and quantum signal processing.**

Keywords- Second harmonic generation; Fundamental modes phase matching; Plasmonic waveguide; Microring resonators

I. INTRODUCTION

Second harmonic generation (SHG) induced by second-order ($\chi^{(2)}$) optical nonlinearities has attracted much attention in recent years for its potential applications in the area of all-optical signal processing such as wavelength conversion [1], optical switch [2], etc. Phase matching conditions (PMCs) are vital to the conversion efficiency of the nonlinear optical process. Benefiting from the flexible geometric structure and tight mode profile, optical waveguides are potential platform for efficient SHG [3].

Over the last few decades, plasmonic waveguides have attracted great research interests in the area of nonlinear photonics due to their extraordinary abilities to break through traditional optical diffraction limits [4]. At present, some waveguides that operate in the near-infrared (NIR) wavelength region have been extensively studied, such as the waveguide combined a second-order nonlinear material lithium niobate ($LiNbO_3$) and a plasmonic structure [5-7]. Furthermore, the conversion efficiency can be significantly improved by employing a highly nonlinear polymer [8, 9]. It should be noted that, currently, most of the SHG waveguides are based on quasi-phase matching (QPM) or intermodal-phase matching (IMPM) techniques. However, the QPM usually relies on the iron exchange or grating structure which complicates the fabrication process. For IMPM, the generated harmonic is in the form of higher-order mode (HOM) which is difficult for manipulation. Particularly, it is inferior for the application such as photon pair generation since an additional mode convertor is required to produce the target pump mode.

Recently, plasmonic waveguides that operate in the mid-infrared (MIR) have received much attention for its wide range of applications in sensing and imaging [10]. However, the photodetectors operating in the MIR wavelength usually show much higher noise and lower sensitivity. Therefore, upconverting the MIR signal to NIR through optical parametric process for detection is highly desired. Transparent conductive oxide (TCO), such as indium cadmium oxide (CdO) and indium tin oxide (ITO) have gathered significant attentions as alternative materials for plasmonic. This is because the dispersion relation can be easily tailored through their carrier concentrations [12]. Such property is favorable for constructing optical sensors and modulator. Furthermore, it brings a chance for a new kind of phase matching technique for SHG.

In this paper, by using the unique dispersion relation of CdO, a dielectric-loaded SHG waveguide with PMC between two fundamental modes are proposed. At MIR, the CdO behaves as metal and supports the plasmonic mode. While at NIR, it becomes a dielectric material with refractive index higher than the substrate and thus a photonic mode can be formed. By optimizing the carrier density and waveguide geometry, these two modes can be perfectly phase-matched for SHG. Besides the straight waveguide, a microring resonator (MRR) is employed to further enhance the conversion efficiency.

978-1-7281-0426-3/19/$31.00 ©2019 IEEE

II. Second Harmonic Generation in Waveguide

A. Theory and Waveguide Design

The proposed waveguide structure is shown in Fig. 1(a), where h and w represent the height and width of the polymer waveguide. The considered polymer is the same as the one used in [8] , and its second order nonlinear susceptibility ($\chi^{(2)}$) is 619.4 pm/V. The refractive indices of the polymer at 3100nm and 1550nm are 1.477597 and 1.479017 [13], respectively. The substrate is composed of CdO and the whole device is surrounded by air. According to the Drude model [12], the dielectric constant of CdO is given by

$$\varepsilon=\varepsilon'+j\varepsilon''=\varepsilon_\infty-\frac{\omega_p}{\omega(\omega+j\gamma)} \tag{1}$$

$$\omega_p=\sqrt{\frac{ne^2}{m_{eff}\varepsilon_0}} \tag{2}$$

where ε' and ε'' are the real and imaginary parts of the permittivity, respectively. ε_∞ is the high frequency dielectric constant, ω_p is the plasma frequency, ω is the angular frequency of the light wave, γ is the damping degree, n is the electron density, e is the electron charge, ε_0 is the vacuum absolute permittivity, and m_{eff} ($m_{eff}=km_0$) is the effective mass of the electron, where m_0 is the mass of the free electron. In our work, $n=6\times10^{26}$ m^{-3}, $e=1.602\times10^{-19}$ C, $\varepsilon_0=8.854\times10^{-12}$ F/m, $\gamma=2.92\times10^{13}$ rad/s, $m_{eff}=1.823e^{-31}$ kg and $\varepsilon_\infty=5.5$ F/m, respectively. Fig. 1(b) shows the variation curve of the CdO permittivity with wavelength.

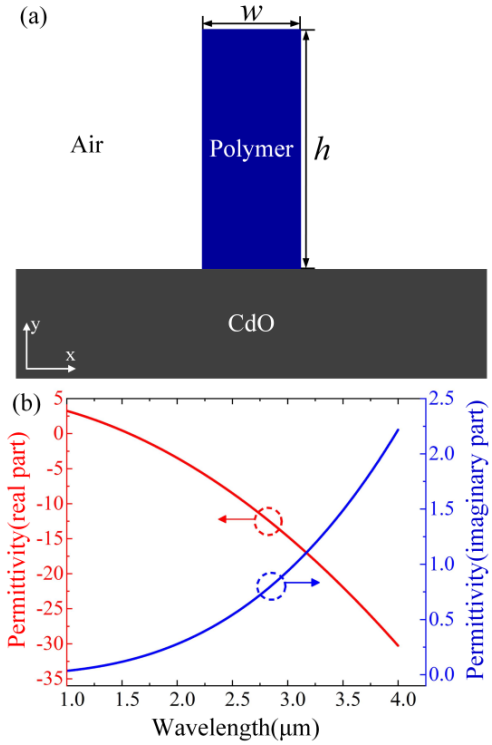

Figure 1. " (a) The cross-section view of the proposed waveguide; (b) CdO permittivity versus wavelength.

According to Fig. 1(b), it can be found that the real part of the dielectric constant in NIR is positive. In this case, CdO behaves as dielectric material thus supporting photonic modes in NIR. When the wavelength increases to ~1650 nm, the real part of the dielectric constant becomes negative thus supporting plasmonic modes. Here the propagation modes of 3100 nm and 1550 nm in the waveguide are considered. By numerical calculation through finite element method software, the width and height of the polymer waveguide are mediated to satisfy the PMC for SHG. With the waveguide width w=858 nm and h=2000 nm, the effective indices of FF and SHF are 1.3105+0.00685i and 1.3106+0.00059i, respectively. The corresponding electric mode profiles of the fundamental modes at 3100 nm and 1550 nm are plotted in Fig. 2(a) and (b).

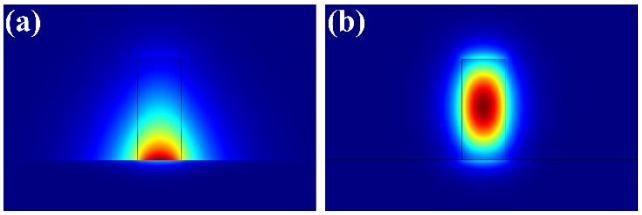

Figure 2. " Electric mode profiles of (a) plasmonic mode at 3100nm and (b) photonic mode at 1550nm with h=2000 nm and w=858 nm.

In addition to PMCs, high efficient SHG requires high nonlinear coupling coefficients (NCCs) between the pump and harmonic modes which are determined by the nonlinear susceptibility and mode overlap. The definition of the NCC is given in [14]

$$C_X=\varepsilon_0\iint_{A_{NL}}\chi^{(2)}:\vec{E}_2\vec{E}_1^*\cdot\vec{E}_1^*dxdy \tag{3}$$

where E_1 and E_2 are the normalized electric fields at the modes of FF and SHF, respectively.

According to our calculation, the NCC in the proposed waveguide is as high as 49.192 ps·m^{-1}·W$^{-1/2}$. It should be noted that different PMCs can be achieved by adjusting the waveguide geometric parameters as the black curve shown in Fig. 3. It can be seen that the NCC values can maintained above 48 ps·m^{-1}·W$^{-1/2}$ in the waveguide height from 1600 nm to 2200 nm.

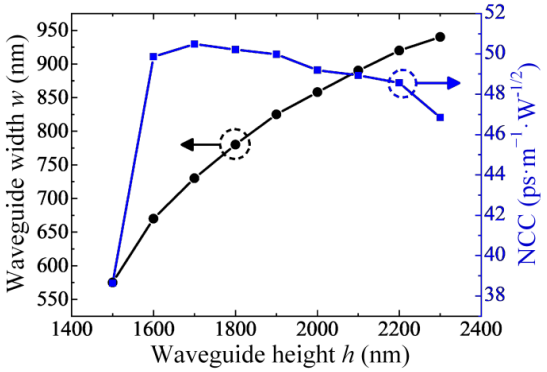

Figure 3. " The waveguide width and corresponding NCC with respect to the waveguide height.

B. *Performance of SHG in the Proposed Waveguide*

For the SHG process, the performance is investigated by solving the coupled-mode equations [9]

$$\frac{\partial A_{FF}}{\partial z} = -\frac{1}{2}\alpha_{FF} A_{FF} + i\frac{\omega_{FF}}{4} C_X A_{FF}^{*} A_{SHF} \exp(i\Delta\beta z) \quad (4)$$

$$\frac{\partial A_{SHF}}{\partial z} = -\frac{1}{2}\alpha_{SHF} A_{SHF} + i\frac{\omega_{FF}}{4} C_X{}^{*} A_{FF} A_{FF} \exp(-i\Delta\beta z) \quad (5)$$

where A_{FF} and A_{SHF} are the normalized mode amplitudes of pump and harmonic, respectively. α_{FF} and α_{SHF} are the loss coefficients of pump and harmonic and $\Delta\beta$ is the phase mismatch. Under the condition of h=2000 nm and w=858 nm, α_{FF}=0.12 dB·μm^{-1}, α_{SHF}=0.021 dB·μm^{-1} and $\Delta\beta$=0 are calculated, respectively. The conversion efficiency of SHG is defined as follow

$$\eta = \frac{P_2(L)}{P_1(0)} \quad (6)$$

where $P_1(0)$ is the input pump power, L is the waveguide length and $P_2(L)$ is the corresponding output power of SH.

With 1W pump power, the SHG performance is shown in Fig. 4. It can be found that the SH power reaches the peak power of 0.0417 W with the propagation length of 92.3 μm. After the conversion peak, the pump power becomes weak and the nonlinear gain is insufficient to compensate the linear loss of SH resulting in the decay of conversion with longer waveguide.

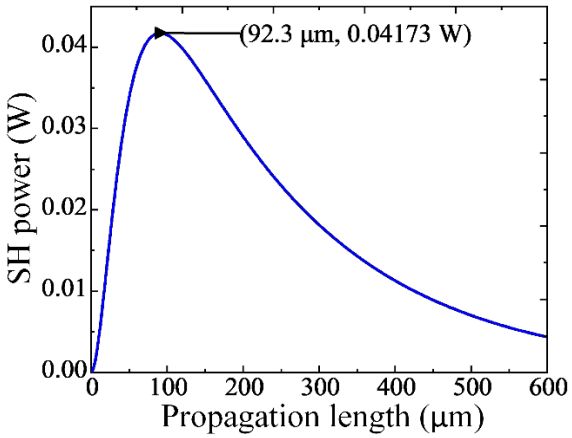

Figure 4. " SH power along propagation length in the waveguide with 1 W CW pump power.

The fabrication-error can induce degradation to the phase mismatch $\Delta\beta$. Fig. 5 depicts the conversion efficiency with respect to different phase mismatch $\Delta\beta$ along propagation distance in waveguide. Considering 3 dB conversion efficiency deviation, the phase mismatch is within the range of $\pm 5.02\times10^{4}$ m^{-1}. Such phase mismatch corresponds to the variation of waveguide height, width and pump wavelength of ±280 nm, ±113 nm and ±125 nm, respectively. Therefore, the proposed waveguide possesses a large fabrication-error tolerance.

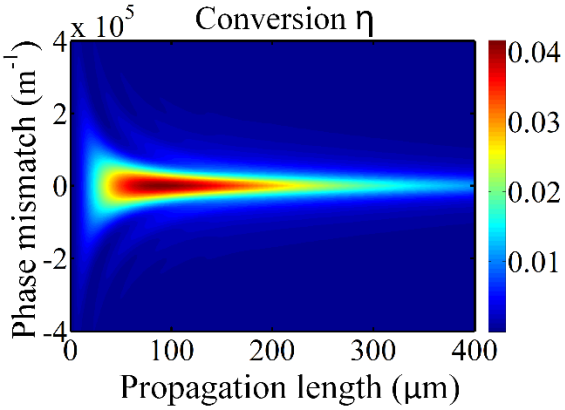

Figure 5. " The conversion efficiency with different phase mismatch along propagation length.

III." SECOND HARMONIC GENERATION ENHANCEMENT IN MICRORING RESONATOR

A. *Theory and Microring Resonator Design*

To further enhance SHG, the structure of MRR based on the proposed waveguide is designed as shown in Fig. 6(a) and (b). The pump in the bus waveguide is coupled to the ring through a coupling gap defined as g. The radius of the ring is R.

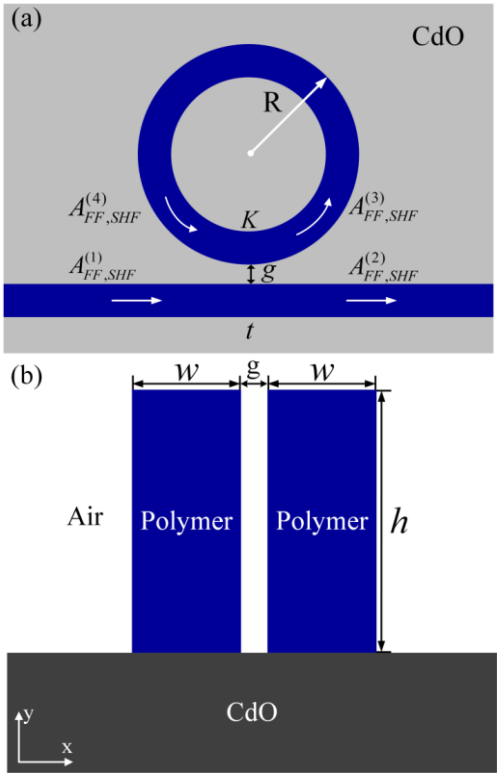

Figure 6. " The cross-section view of the proposed MMR along (a) x-z and (b) x-y planes.

The resonance condition can be satisfied by choose the appropriate radius of the ring to enhance the SHG and the resonance condition for FF can be defined as follows [15]

$$m_{FF} = k_{FF} n_{eff} R \tag{7}$$

where m_{FF} is the azimuth number of resonance and is an integer respectively. k_{FF} is propagation constant, and n_{eff} is the effective refractive index at FF, respectively. Considering the nearest integer m_{FF}, the radius R=3 μm is finally chosen with m_{FF} =8.

In the coupling region as shown in Fig. 6(a), the boundary condition in the MRR can be given by the following equation [15]

$$A^{(2)}_{FF,SHF} = \mathrm{t}_{FF,SHF} A^{(1)}_{FF,SHF} + iK_{FF,SHF} A^{(4)}_{FF,SHF} \tag{8}$$

$$A^{(3)}_{FF,SHF} = iK_{FF,SHF} A^{(1)}_{FF,SHF} + \mathrm{t}_{FF,SHF} A^{(4)}_{FF,SHF} \tag{9}$$

where complex mode amplitudes A at FF and SHF are normalized, respectively. t and K are the optical field transmission coefficients and coupling coefficients, and they satisfy $|K|^2+|t|^2=1$, respectively. Here, K can be calculated by the coupled mode theory [16].

With all the other parameters of the MRR being determined, the transmission coefficients of t and coupling coefficients of K are only related to the coupling gap distance g between the bus waveguide and the ring. Fig. 6(a) depicts the transmission coefficients at FF and SHF with respect to different gaps. It can be clearly seen that t_{SHF} is usually larger than t_{FF}. Then, the transmission coefficients under the critical coupling conditions of FF (t_{FF}) and SHF (t_{SHF}) are obtained, respectively. As is shown in Fig. 7, $t_{FF} = \exp(-\pi\alpha_{FF}R) = 0.7697$ corresponds to the gap of 265.5 nm, and $t_{SHF} = \exp(-\pi\alpha_{SHF}R) = 0.9561$ corresponds to the gap of 200 nm. It should be noted that the critical coupling points at FF and SHF are different.

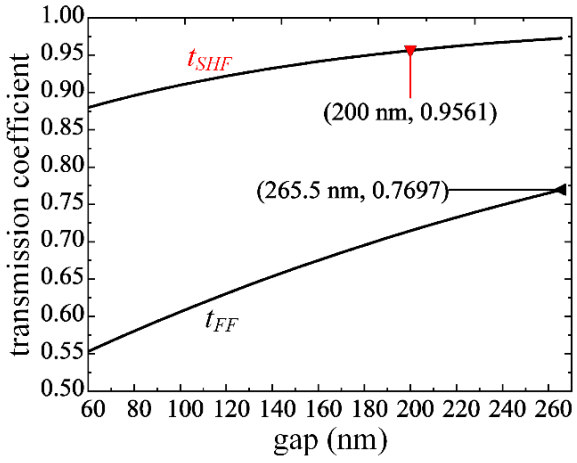

Figure 7. " Transmission coefficients at FF (black line) and SHF (red line) versus the gap.

B. Enhancement of SHG in the microring resonator

Firstly, the gap of g=110 nm is chosen and the corresponding transmission coefficients are t_{FF}= 0.6185 and t_{SHF}=0.9160, respectively. The SHG performance in the MMR is investigated by solving Eq. (4) and (5) together with the boundary conditions Eq. (8) and (9).

With pump power of 100 mW, the output power of SH is 5.316 mW corresponding to a SHG efficiency of 5.316%. For the intracavity power, the SH power reaches a steady value of 27.73 mW after ~74 roundtrips, as shown in Fig. 8(a). The output SH power with respect to different gaps is illustrated in Fig. 8(b). It can be seen that the maximum of SH power in the bus waveguide is 6.16 mW with gap of 190 nm, which is quite close to the critical coupling condition for SH mode. The conversion at critical coupling condition for FF is 5.5 mW corresponding to g=265.5 nm. It is obvious that the SH conversion efficiency in the proposed MRR can be enhanced compared to the straight waveguide.

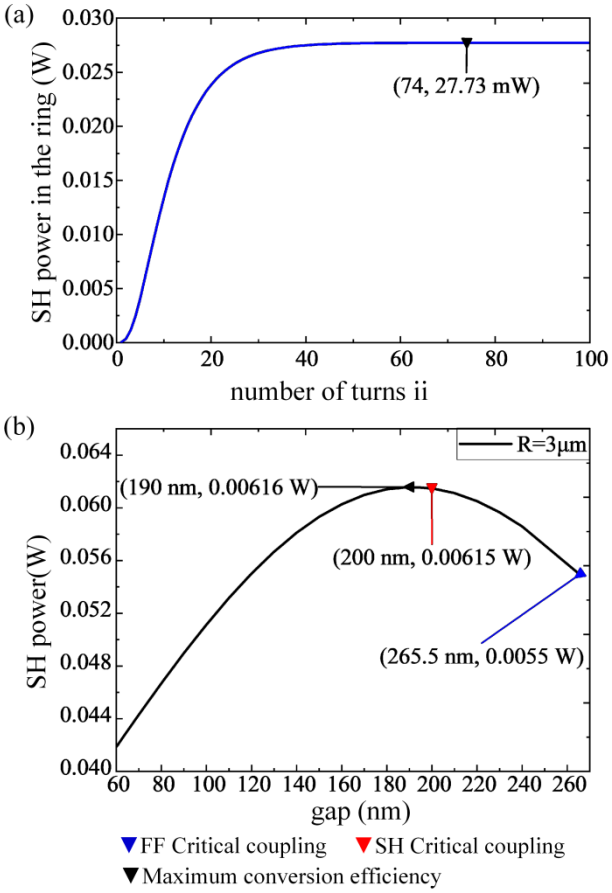

Figure 8. " (a)SH power in the ring versus the number of turns ii.(b)The output SH power with different gaps

With R and g of the MRR fixed to 3.0 μm and 110 nm, the output SH power at different pump power is shown in Fig. 9(a). It can be found that both the output SH power and the SH conversion efficiency are improved with increasing the input pump power. Particularly, when the pump power varies from 100 mW to 1 W, the SH conversion efficiency is rapidly

improved. With pump power of 1 W, the SH conversion efficiency is calculated to be 26.05% in the MRR, which is 6 times that in the straight waveguide. Fig. 9(b) depicts the output SH power with respect to different gaps at different radius of the MRR when the pump power is fixed to 1W. The conversion efficiency increases with the radius decreasing due to lower total loss of MRR.

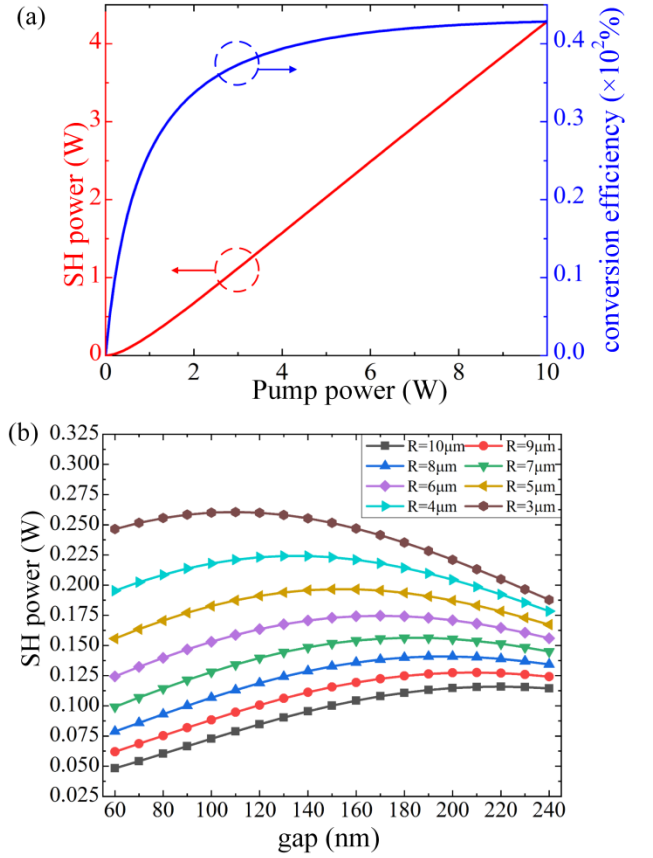

Figure 9. [n] (a) Output SH power (red line) and SH conversion efficiency (blue line) versus different pump powers.(b)With pump power of 1 W, the SH power variation with gap at different radii (*R* is from 3 μm to 10 μm)

IV.[n] DISCUSSION AND CONCLUSION

In summary, a dielectric-loaded waveguide for SHG from MIR to NIR is proposed. Leveraging the unique dispersion relation of CdO, the PMC for SHG can be satisfied between the fundamental plasmonic mode at FF and photonic mode at SHF, respectively. According to numerical simulation results, the SH conversion efficiency of 4.173% can be obtained with waveguide length of 92.3 μm under 1 W pump power. To further enhance the conversion efficiency, a MRR is designed and optimized based on the proposed waveguide. It is shown that the required pump power can be much lower compare to the straight waveguide. SH conversion up to 6.16% can be obtained with pump power of only 100 mW. In addition, the SHG conversion efficiency can be improved by increasing pump power. The proposed waveguide can find potential applications in the areas of MIR to NIR upconversion detection and quantum signal processing.

REFERENCES

[1][n] S. Zlatanovic, J. S. Park, et al., "Mid-infrared wavelength conversion in silicon waveguides using ultracompact telecom-band-derived pump source," Nat. Photonics 4, 561–564 (2010).

[2][n] S. Farazi and A. Zarifkar, "A Low-Power Optical Nanoswitch Based on XPM-Enhanced Second Harmonic Generation," J. Lightwave Technol. 35, 1988-1994 (2017)

[3][n] M. Cazzanelli, F. Bianco, et al., "Second-harmonic generation in silicon waveguides strained by silicon nitride," Nat. Mater. 11(2), 148–154 (2011).

[4][n] M. Kauranen and A. V. Zayats, "Nonlinear plasmonics," Nat. Photonics 6(11), 737–748 (2012).

[5][n] S. B. Hasan, C. Rockstuhl, T. Pertsch, and F. Lederer, "Second-order nonlinear frequency conversion processes in plasmonic slot waveguides," J. Opt. Soc. Am. B 29(7), 1606–1611 (2012)

[6][n] B. N. Carnio and A. Y. Elezzabi, "Second harmonic generation in metal-$LiNbO_3$-metal and $LiNbO_3$ hybrid-plasmonic waveguides," Opt. Express 26, 26283-26291 (2018)

[7][n] F. F. Lu, T. Li, X. P. Hu, Q. Q. Cheng, S. N. Zhu, and Y. Y. Zhu, "Efficient second-harmonic generation in nonlinear plasmonic waveguide," Opt. Lett. 36(17), 3371–3373 (2011).

[8][n] J. Zhang, E. Cassan, D. Gao, and X. Zhang, "Highly efficient phase-matched second harmonic generation using an asymmetric plasmonic slot waveguide configuration in hybrid polymer-silicon photonics," Opt. Express 21(12), 14876–14887 (2013).

[9][n] T. Huang, P. Moteng Tagne, and S. Fu, "Efficient second harmonic generation in internal asymmetric plasmonic slot waveguide," Opt. Express 24, 9706-9714 (2016).

[10][n] T. Huang et al., "Photon–Plasmon Coupling for Fundamental-Mode Phase-Matched Third Harmonic and Triplet Photon Generation," in Journal of Lightwave Technology, vol. 36, no. 18, pp. 3892-3897, 15 Sept.15, 2018. doi: 10.1109/JLT.2018.2851998

[11][n] B. Kumari, A. Barh, R. K. Varshney, B. P. Pal, "Silicon-on-nitride slot waveguide: A promising platform as mid-IR trace gas sensor," Sensors and Actuators B-Chemical, vol. 236, pp. 759-764, 2016.

[12][n] Y. Yang, K. Kelley, E. Sachet, S. Campione, T. S. Luk, J. P. Maria, M. B. Sinclair, and I. Brener, "Femtosecond optical polarization switching using a cadmium oxide-based perfect absorber," *Nat. Photon.*, vol. 11, no. 6, pp. 390-395, 2017.

[13][n] S. Kim and M. Qi, "Broadband second-harmonic phase-matching in dispersion engineered slot waveguides," Opt. Express 24, 773-786 (2016)

[14][n] F. F. Lu, T. Li, J. Xu, Z. D. Xie, L. Li, S. N. Zhu, and Y. Y. Zhu, "Surface plasmon polariton enhanced by optical parametric amplification in nonlinear hybrid waveguide," Opt. Express 19(4), 2858–2865 (2011)

[15][n] J. Zhang, E. Cassan, and X. Zhang, "Enhanced mid-to-near-infrared second harmonic generation in silicon plasmonic microring resonators with low pump power," Photon. Res. 2, 143-149 (2014).

[16][n] K. Okamoto, *Fundamentals of Optical Waveguides* (Academic,2010).